turn, the computed quasi-one-dimensional gain profile should also be a reasonable average of the actual two-dimensional results. Similar trends occur for throat heights = 0.3 mm and 2.0 mm with γ variations between 1.33 and 1.40.[11]

The following conclusion is apparent. In comparison to a completely sharp throat ($R_c = 0$), the present results indicate that gain and maximum available power are reduced on the order of 0–15% (depending on the particular case) by complete rounding of the throat (on both the subsonic and supersonic sides). Whether the manufacturing and alignment advantages of round throats outweighs this relatively small reduction in laser performance depends upon the individual application. However, the purpose of this Note has been to present data which will be helpful in making such decisions.

References

[1] Gerry, E. T., "Gasdynamic Lasers," AIAA Paper 71-23, New York, 1971.

[2] Hertzberg, A., Johnston, E. W., and Ahlstrom, H. G., "Photon Generators and Engines for Laser Power Transmission," AIAA Paper 71-106, New York, 1971.

[3] Meinzer, R. A., "Experimental GDL Investigation," AIAA Paper 71-25, New York, 1971.

[4] Anderson, J. D. Jr. and Winkler, E. M., "High Temperature Aerodynamics with Electromagnetic Radiation," *Proceedings of the IEEE*, Vol. 59, No. 4, April 1971, pp. 651–658.

[5] Greenberg, R. A., Schneiderman, A. M., Ahouse, D. R., and Parmentier, E. M., "Rapid Expansion Nozzles for Gas Dynamic Lasers," AMP 314, AVCO Everett Research Laboratory, Dec. 1970, Everrett, Mass.

[6] Wagner, J. L., "A Cold Flow Field Experimental Study Associated with a Two-Dimensional Multiple Nozzle," NOLTR 71-78, July 1971, Naval Ordnance Laboratory, Silver Springs, Md.

[7] Anderson, J. D. Jr., "Time-Dependent Analysis of Population Inversions in an Expanding Gas," *The Physics of Fluids*, Vol. 13, No. 8, Aug, 1970, pp. 1983–1989.

[8] Anderson, J. D. Jr., "Numerical Experiments Associated with Gas Dynamic Lasers," NOLTR 70-198, Sept. 1970, Naval Ordnance Laboratory, Silver Springs, Md.

[9] Lee, G. and Gowen, F. R., "Gain of CO_2 Gasdynamic Lasers," *Applied Physics Letters*, Vol. 18, No. 6, March 1971, pp. 237–239.

[10] Anderson, J. D. Jr., Humphrey, R. L., Vamos, J. S., Plummer, M. J., and Jensen, R. E., "Population Inversions in an Expanding Gas: Theory and Experiment," *The Physics of Fluids*, Vol. 14, No. 12, Dec. 1971, pp. 2620–2624.

[11] Wagner, J. L. and Anderson, J. D. Jr., "An Analytical Investigation of the Effect of Nozzle Throat Radius of Curvature on Gasdynamic Laser Gain." NOLTR 72-5, Naval Ordnance Laboratory, Silver Springs, Md.

Prediction of Tank Pressure History in a Blowdown Propellant Feed System

GILBERT F. PASLEY*

Hughes Aircraft Company, El Segundo, Calif.

Nomenclature

d = propellant tank diameter
g = acceleration of gravity
Gr = Grashof number
H = heat transfer coefficient
K = thermal conductivity
m = mass
Nu = Nusselt number
Pr = Prandtl number
Q = heat content

Subscripts

d = diameter (characteristic length)
p = propellant
w = tank wall

Received November 19, 1971; revision received February 22, 1972.

Index categories: Spacecraft Propulsion Systems Integration; Spacecraft Attitude Dynamics and Control; and Liquid Rocket Engines.

* Member of Technical Staff, Space and Communications Group. Member AIAA.

Introduction

MANY current spacecraft utilize the same tankage for propellant and pressurant to avoid the complexity of a separate pressurant tank and, hence, improve reliability; therefore, the initial tank pressure decays as propellant is consumed. Since the flowrate to the rocket engine decreases as the tank pressure decreases, the impulse available at any time prior to propellant depletion is dependent upon the tank pressure history. The observed pressure decay has caused this type of design to be designated the "blowdown type" of propellant supply system, although none of the pressurant is expelled from the tank.

It has been shown[1] that the rate of heat transfer from a sphere to the contained fluid could be accurately predicted by an existing empirical correlation. The same correlation is applied to the blowdown type of propulsion system design to predict transient pressure histories and, hence, the total impulse available at any time.

Discussion

The propellant supply systems shown schematically in Fig. 1 are typical blowdown designs. The propellant leaves the tank at the instantaneous rate of $\dot{m}_p$, and heat is transferred to the pressurant from the pressurant tank wall and propellant surface at the instantaneous rates, $\dot{Q}_w$ and $\dot{Q}_p$, respectively. Since the derivation of the equations describing the controlling thermodynamic processes is similar to that presented in Ref. 1, the derivation will not be given. However, a list of the applicable assumption is in order. They are: 1) the internal energy of the pressurant is a function of temperature only; 2) the pressurant behaves as a perfect gas (a good assumption at the relative low pressures of 20 atmospheres encountered in most designs); 3) specific impulse, flow controlling orifice

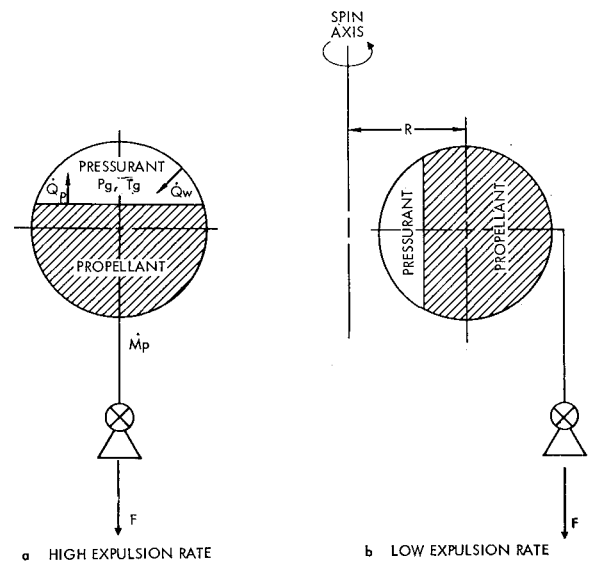

Fig. 1 Blowdown propellant supply system schematics.

coefficient, and thrust coefficient are constant, since they are only weakly dependent upon flow rate; 4) since the propellant tanks operate in a vacuum with aluminized mylar radiation shielding, their external surfaces are adiabatic; 5) the tank wall exposed to the propellant is the same temperature as the propellant; and 6) the propellant has infinite thermal conductivity.

The determination of the heat transfer coefficient, H, is the key to the development of a general set of equations which can be used to describe tank pressure history at various propellant usage rates. Although data on free-convection heat transfer to a gas in a sphere are unavailable, Reference 2 presents a relationship derived from the results of "experiments on free-convection heat transfer from the surface of a sphere to a fluid filling the interior ... Alcohol, glycol, and water were used as fluids, and a range of 3×10^8 to 5×10^{11} of the product Gr_dPr was covered." The equation is

$$Nu_d = Hd/K = 0.098\,(Gr_dPr)^{0.345} \quad (1)$$

Since the Grashof number, Gr_d, is directly dependent on the acceleration field, changes in heat transfer resulting from the altered free-convection fluid flow during variable accelerations is accounted for in the results. Since the cases under consideration involve relatively high acceleration fields (approximately one-tenth axial g for the high thrust system and 3 radial g for the low thrust system shown in Table 1), Eq. 1 is expected to be a valid correlation for these applications. Although an "exact" theory is not available to allow direct comparison with the empirical correlation of data represented by Eq. 1, it has been shown to predict actual inflight data with excellent accuracy (Ref. 1) and there is no reason to expect that it would not provide equally good predictions in the types of systems discussed herein.

The analysis is substantially simplified if either the expansion process is isothermal or the heat transfer coefficient, H, can be assumed constant. References 3 and 4 discuss the restrictions imposed on the analysis when H is assumed to be at either of its limits, zero or infinity. The $H = 0$ case corresponds physically to an adiabatic gas, whereas the $H = \infty$ case requires that the pressurant storage vessel, the propellant, and the gas be at the same temperature during the entire expulsion period.

To assess the importance of variations in H on the available total impulse, four cases (isothermal, $H = 0$, finite, and infinite) were computed for two spacecraft configurations. The first configuration analyzed was a high thrust, high propellant weight system as described in Table 1. This system is typical of liquid propellant orbit injection designs. The second configuration studied was a low thrust, low propellant weight system with the parameters shown in Table 1. This system is typical of orbit adjust systems used on communication satellites. Both systems used nitrogen, hydrazine, and titanium as pressurant, propellant, and tank material, respectively.

Table 1 Typical blowndown system design parameters

Parameter	High thrust system	Low thrust system
Spacecraft mass[a], kg	453	[b]
Propellant mass[a], kg	90.7	22.7
Tank pressure[a], n/m^2	2.07×10^6	2.07×10^6
Tank temperature[a], °C	21.1	21.1
Chamber pressure[a], n/m^2	6.89×10^5	6.89×10^5
Thrust[a], n	444	22.2
Specific impulse, n-sec/kg	463	463
Tank mass, kg	3.71	1.47
Tank diameter, m	0.636	0.401
Spacecraft spin speed, rad/sec	[b]	6.3
R [Fig. 1b], m	[b]	0.61
Nominal expulsion time (t_n) sec	743	3,550
Total impulse available, n-sec	20.4×10^4	5.11×10^4

[a] Initial condition.
[b] Not applicable.

Results and Conclusions

The total impulse data predicted by the equations incorporating the various values of H were normalized by dividing by the total available impulse shown in Table 1 (the expulsion time was also divided by the "nominal" value shown in Table 1). When this was done, it was found that the high and low flowrate curves resulting from the use of Eq. 1 were coincident, so that one curve in Fig. 2 represents both results.

It was also found that the isothermal and $H = \infty$ cases predict the same propellant expulsion time. This is a result of having the propellant and pressurant in the same tankage; i.e., since the weight of propellant is many times that of the gas, the propellant acts as an infinite heat source for the $H = \infty$ case, and the system temperature drops only a few degrees below the isothermal temperature at propellant depletion. Of the two simplifications, the isothermal assumption results in much simpler equations describing system performance and, hence, is recommended for systems operating at low expulsion rates. In actual practice, the propellant is usually withdrawn during relatively short duration burns rather than in the continuous expulsion shown in Fig. 2. This fact makes the isothermal assumption increasingly valid, since the pressurant has sufficient time to come to thermal equilibrium with the propellant between expulsion periods.

As seen in Fig. 2, however, at high expulsion rates, the use of the isothermal assumption rather than the true heat transfer coefficient from Eq. 1 results in a propellant depletion time which is approximately 5% below the true time. The significance of an error of this magnitude must be evaluated for each spacecraft. However, as the expulsion rate increases, the adiabatic ($H = 0$) case is approached; hence, from Fig. 2, for rapid expulsion rates, an error of 19% is possible if the isothermal assumption is used.

It should be noted that the assumption of constant specific impulse used herein is only an approximation. Depending upon the particular thruster design, specific impulse falls as inlet pressure decays. It follows then that, since total impulse is directly related to specific impulse, total impulse will be dependent upon the tank pressure history; i.e., that set of circumstances which results in the highest average tank pressure will produce the highest total impulse. Hence, it may be advantageous to supply pressurant heaters to high expulsion rate systems to achieve maximum available impulse.

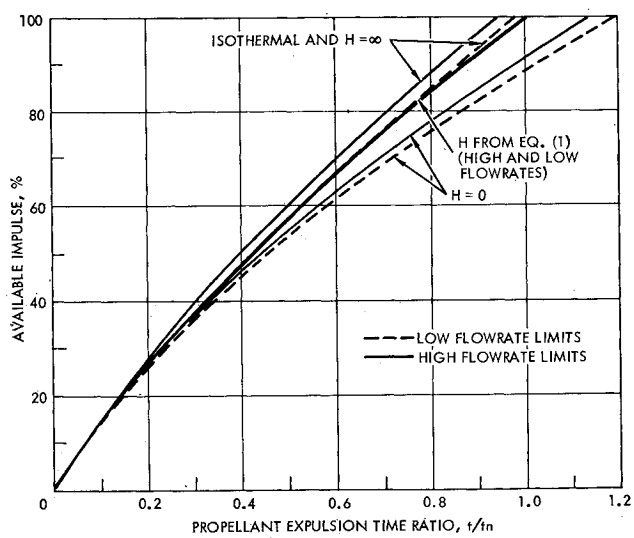

Fig. 2 Total impulse histories vs propellant expulsion rate.

References

[1] Pasley, G. F., "Optimization of Stored Pressurant Supply for Liquid Propulsion Systems," *Journal of Spacecraft and Rockets*, Vol. 7, No. 12, Dec. 1970, pp. 1478–1480.

[2] Eckert, E. R. G. and Drake, Jr., R. M., *Heat and Mass Transfer*, 2nd ed., McGraw-Hill, New York, 1959, pp. 324–325.

[3] "Design Guide for Pressurized Gas Systems," NASA Contract NAS7-388, March 1966, ITT Research Inst., Chicago, Ill.

[4] *Pressurization Systems Design Guide*, Vol. I, Rept. 2736, Dec. 1965. Aerojet-General Corp., Von Kármán Center, Azusa, Calif.

Mixed-Mode Propulsion: Optimum Burn Profile for Two-Mode Systems

ROBERT SALKELD*
System Development Corporation
Santa Monica, Calif.
AND
ROBERT S. SKULSKY†
McDonnell-Douglas Corporation
Huntington Beach, Calif.

Nomenclature

C = constant, $\rho_2(u_2 - u_1)/(\rho_1 - \rho_2)$
m = mass
u = exhaust velocity
$\bar{u}$ = average u for both modes operating concurrently
V = volume of propellant burned
v = vehicle velocity
ρ = propellant bulk density
$\bar{\rho}$ = average ρ for both modes operating concurrently

Subscripts

0, 1, 2, f = initial, mode-1, mode-2, final

Introduction

It has been pointed out[1] that combining different propulsion modes in the same stage promises improved vehicle performance, cost and operating characteristics, and may make a reusable one-stage-to-orbit machine feasible. Reference 1 assumes a purely sequential burn for the two-mode system. Under this assumption, the analysis indicates that the higher density mode should be operated first. The question is left open, however, whether sequential or some form of overlapping burn profile constitutes the true optimum for maximizing ideal Δv. The purpose of this analysis is to answer that question.

Analysis

Generalization of the ideal rocket equation

Consider a mixed-mode rocket stage having a given initial mass m_0, in which the modes can be operated concurrently at arbitrarily varying flow rates. Thus,

$$\bar{\rho} = \bar{\rho}(V) \tag{1}$$

$$\bar{u} = \bar{u}(\bar{\rho}(V)) \tag{2}$$

Received December 20, 1971; revision received February 11, 1972. The authors are indebted to J. D. Riley, McDonnell-Douglas for his mathematical guidance and verification

Index categories: Launch Vehicle Systems; Liquid Rocket Engines; Hypersonic Airbreathing Propulsion.

* Special Assistant to the Chairman. Associate Fellow AIAA.
† Senior Engineer-Scientist. Member AIAA.

Equation (1) represents the burn profile, and Eq. (2) represents the specific functional dependency of $\bar{u}$ upon $\bar{\rho}$.

Since the purpose of this analysis is to present as simply as possible an initial derivation of the optimum burn profile, consideration of gravity and drag forces and more sophisticated formulations of the rocket equation[2] will not be included here. For point-mass analysis, conservation of momentum gives

$$\bar{u}\bar{\rho}dV = \left[m_0 - \int_0^V \bar{\rho}(\tilde{V})d\tilde{V}\right]dv \tag{3}$$

Substituting Eqs. (1) and (2) and integrating

$$\Delta v = \int_0^{V_f} \frac{\bar{\rho}(V)\bar{u}(\bar{\rho}(V))dV}{m_0 - \int_0^V \bar{\rho}(\tilde{V})d\tilde{V}} \tag{4}$$

which is a generalized form of the ideal rocket equation where $\bar{\rho}$ and $\bar{u}$ are no longer constant as in the more familiar classical single-mode case.

Optimization for the two-mode case

To maximize Δv in Eq. (4), it is first necessary to specify the function $\bar{u}[\bar{\rho}(V)]$. This is done by writing the expressions for $\bar{\rho}$ and $\bar{u}$ for the two-mode case,

$$\bar{\rho} = (\dot{m}_1 + \dot{m}_2)/(\dot{m}_i/\rho_1 + \dot{m}_2/\rho_2) \tag{5}$$

$$\bar{u} = (\dot{m}_1 u_2 + \dot{m}_2 u_2)/(\dot{m}_1 + \dot{m}_2) \tag{6}$$

and solving simultaneously to obtain

$$\bar{u} = u_1 + C[(\rho_1/\bar{\rho}) - 1] \tag{7}$$

Now, if we let

$$m = m_0 - \int_0^V \bar{\rho}(V)dV \tag{8}$$

and substitute Eqs. (7) and (8) in Eq. (4), then

$$\Delta v = (C - u_1)\int_{m_0}^{m_f} \frac{dm}{m} + \rho_1 C \int_0^{V_f} \frac{dV}{m} \tag{9}$$

and this becomes upon integration of the first term,

$$\Delta v = (C - u_1)\log_e(m_f/m_0) + \rho_1 C \int_0^{V_f} \frac{dV}{m} \tag{10}$$

which is the generalized ideal rocket equation for the two-mode case.

If the optimum burn profile is continuous, then it should be possible to determine it by applying the calculus of variations to Eq. (10), which can be written

$$\Delta v = \text{constant} + \rho_1 C \int_0^{V_f} F(V, m)dV \tag{10a}$$

Application of calculus of variations is possible only where all variables are continuous and possess continuous first and second derivatives. To define extremals, it is necessary to satisfy the Euler-Lagrange equation which in this case reduces to

$$-\partial F/\partial m = 0 \tag{11}$$

Substituting Eq. (10a) in Eq. (11) and differentiating,

$$-\rho_1 C/m^2 = 0 \tag{12}$$

which requires $m^2 \to \infty$. This is a contradiction which implies that there exists no continuous solution within the limits ρ_1 and ρ_2. Thus, if an optimum solution exists (and Ref. 1 proves that it can), then that solution must involve a discontinuous burn profile.

Applying a more general approach to maximize Δv in Eq. (10), m in the second term of Eq. (10) must be taken as small as possible and still satisfy the boundary conditions of m_0 and m_f. As shown in Fig. 1, the m history must lie between the limits of the straight line curves whose slopes are $-\rho_1$ and $-\rho_2$. Regardless of what m_f value is selected it becomes apparent that the smallest m history can be attained only by burning first the higher density (ρ_1) mode and then switching to the lower density (ρ_2) burn only when the lower density slope ($-\rho_2$) will lead to m_f. This is true regardless of the value of m_f so long as m_f lies between the above bounds, as it must.